PNAS RESEARCH ARTICLE | APPLIED PHYSICAL SCIENCES

Interfacial Cherenkov radiation from ultralow-energy electrons

Zheng Gong[a,b], Jialin Chen[a,b,c], Ruoxi Chen[a,b], Xingjian Zhu[d], Chan Wang[a,e], Xinyan Zhang[a,b], Hao Hu[f], Yi Yang[g], Baile Zhang[h,i,1], Hongsheng Chen[a,b,e,j,1], Ido Kaminer[c], and Xiao Lin[a,b,1]

Edited by Hui Cao, Yale University, New Haven, CT; received April 23, 2023; accepted August 11, 2023

Cherenkov radiation occurs only when a charged particle moves with a velocity exceeding the phase velocity of light in that matter. This radiation mechanism creates directional light emission at a wide range of frequencies and could facilitate the development of on-chip light sources except for the hard-to-satisfy requirement for high-energy particles. Creating Cherenkov radiation from low-energy electrons that has no momentum mismatch with light in free space is still a long-standing challenge. Here, we report a mechanism to overcome this challenge by exploiting a combined effect of interfacial Cherenkov radiation and umklapp scattering, namely the constructive interference of light emission from sequential particle–interface interactions with specially designed (umklapp) momentum-shifts. We find that this combined effect is able to create the interfacial Cherenkov radiation from ultralow-energy electrons, with kinetic energies down to the electron-volt scale. Due to the umklapp scattering for the excited high-momentum Bloch modes, the resulting interfacial Cherenkov radiation is uniquely featured with spatially separated apexes for its wave cone and group cone.

Cherenkov radiation | transition radiation | umklapp scattering | photonic crystals

Significance

Cherenkov radiation is fundamentally limited by Cherenkov threshold, since it generally originates from particle-bulk interactions. This fundamental limitation requires the usage of high-energy charged particles for its creation and impedes many promising applications, such as novel on-chip light sources. Recently, interfacial Cherenkov radiation was revealed by engineering the interference of light emission from sequential particle–interface interactions. Here we report the enticing capability of interface-effect-based Cherenkov radiation to overcome the fundamental limitation of Cherenkov threshold for conventional bulk-effect-based Cherenkov radiation. Remarkably, we find the possibility to create threshold-free interfacial Cherenkov radiation with the aid of umklapp scattering. Our work thus may pave the way toward compact on-chip light sources at some desired frequencies (e.g., terahertz or ultraviolet regimes) from low-energy electrons.

Cherenkov radiation (1–7) is a typical type of free-electron radiation that is crucial to many practical applications, ranging from Cherenkov detectors (8–13), light sources (14–16), and medical imaging (17–19), to photodynamic therapy (20–22). These applications are enabled by a unique feature of Cherenkov radiation, namely the capability to create light emission with high directionality at any frequency, given a charged particle moves with a velocity above the Cherenkov threshold (23, 24), which corresponds to the phase velocity of light in the background matter. As fundamentally restricted by the Cherenkov threshold, these applications have to rely on high-energy particles. For example, the kinetic energies of charged particles used in medical imaging and therapy is in the order of mega-electron-volts (MeV) (22); Cherenkov detectors are useful for the identification of high-energy particles generally in the order of giga-eV (GeV) (12, 13). There is a continuous quest to reduce the Cherenkov threshold, with the hope of even creating Cherenkov radiation from slow electrons. Achieving free-electron radiation (e.g., Cherenkov radiation) from slow electrons (16, 25–30) is now an active area of research that is highly sought after and is of special importance, especially for its prospects to boost the development of integrated light sources.

The reduction of Cherenkov threshold generally relies on the usage of high-momentum modes with low phase velocities, such as those in hyperbolic materials (16, 31–40). Such materials are fundamentally limited by losses and nonlocality (32–34). This way, the phase velocity of these hyperbolic modes cannot reduce to absolute zero; nevertheless, it can be orders of magnitude smaller than the speed of light in free space, leading to low-threshold Cherenkov radiation (16, 32). However, these hyperbolic modes, once excited, remain difficult to couple into free space, since they still suffer from severe momentum mismatch with light in free space and would be totally reflected at the material interface. To extract these hyperbolic modes into free space, additional structural design is mandatory, such as the tilting of the optical axis of hyperbolic materials (35), the nanopatterning of hyperbolic materials themselves (36, 37), or the addition of patterned nanostructures on the interface of hyperbolic materials (16, 38). These additional structural designs for outcoupling purposes may deteriorate the properties of originally excited Cherenkov radiation inside hyperbolic materials, such as the unique relation between the Cherenkov angle and the particle velocity, the directionality, and the radiation spectrum. In short, despite the long history of free-electron radiation (41–50), the creation of Cherenkov radiation that has no momentum mismatch with light in free space from slow electrons remains an enticing but challenging goal. Here, we propose a mechanism to achieve this goal using a unique combination: the umklapp scattering and the constructive interference of radiation from many parallel interfaces, namely transition radiation.

Author contributions: Z.G. and X.L. designed research; Z.G. performed research; Z.G., J.C., R.C., X. Zhu, C.W., X. Zhang, H.H., Y.Y., B.Z., H.C., I.K., and X.L. analyzed data; B.Z., H.C., I.K., and X.L. supervised the project; and Z.G. and X.L. wrote the paper.

The authors declare no competing interest.

This article is a PNAS Direct Submission.

[1]To whom correspondence may be addressed. Email: xiaolinzju@zju.edu.cn, hansomchen@zju.edu.cn, or blzhang@ntu.edu.sg.

This article contains supporting information online at https://www.pnas.org/lookup/suppl/doi:10.1073/pnas.2306601120/-/DCSupplemental.

Published September 11, 2023.

Transition radiation (51–54) originates from particle–interface interactions. It is distinct from the conventional bulk Cherenkov radiation originating from particle–bulk interactions. The conventional transition radiation could occur at any electron velocity and is of poor directionality, especially for slow electrons, but inherently momentum-matched with light in free space. Recently, we revealed in ref. 13 that the constructive interference of transition radiation excited by the interaction between relativistic charged particles and many parallel interfaces can effectively form an alternative type of Cherenkov radiation with high directionality. Since this type of effective Cherenkov radiation is induced by particle–interface interactions, we suggest to denote it as interfacial Cherenkov radiation, which intrinsically has no momentum mismatch with light in free space and can thus freely couple into free space. The study of interfacial Cherenkov radiation has already demonstrated its potential in the design of nanophotonic Cherenkov detectors for identifying high-energy particles (13) but is still in its infancy. Whether the interface effect could also be exploited to create the interfacial Cherenkov radiation from slow electrons remains an open question.

In this work, we reveal the possibility of creating interfacial Cherenkov radiation from ultralow-energy electrons. We find that the interfacial Cherenkov radiation is essentially threshold-free since the accompanied umklapp scattering could flexibly shift the momentum of excited high-momentum Bloch modes along the direction of periodicity. While high-momentum Bloch modes in photonic crystals (55–59) were used to reduce the Cherenkov threshold, previous works focused on the discussion of conventional bulk Cherenkov radiation inside photonic crystals (55). Since the umklapp scattering would reshape the wave cone (namely a constant-phase surface), we find that the interfacial Cherenkov radiation is also featured with spatially separated apexes for its wave cone and group cone (related to the crest of light emission or the Cherenkov cone).

We begin with the Huygens construction (60–62) for the wave and group cones of interfacial Cherenkov radiation inside an ideal unbounded 1D photonic crystal in Fig. 1 *A*–*F*. Without loss of generality, the photonic crystal is composed of two transparent dielectrics, such as those with relative permittivities of $\varepsilon_{r,1}$ and $\varepsilon_{r,2}$, respectively. In order to let the electrons safely pass through the photonic crystal, one may drill a tiny hole (14) through the photonic crystal along the electron trajectory. Generally, the Huygens construction for the wave and group cones of Cherenkov radiation is related to four types of velocities, namely the electron

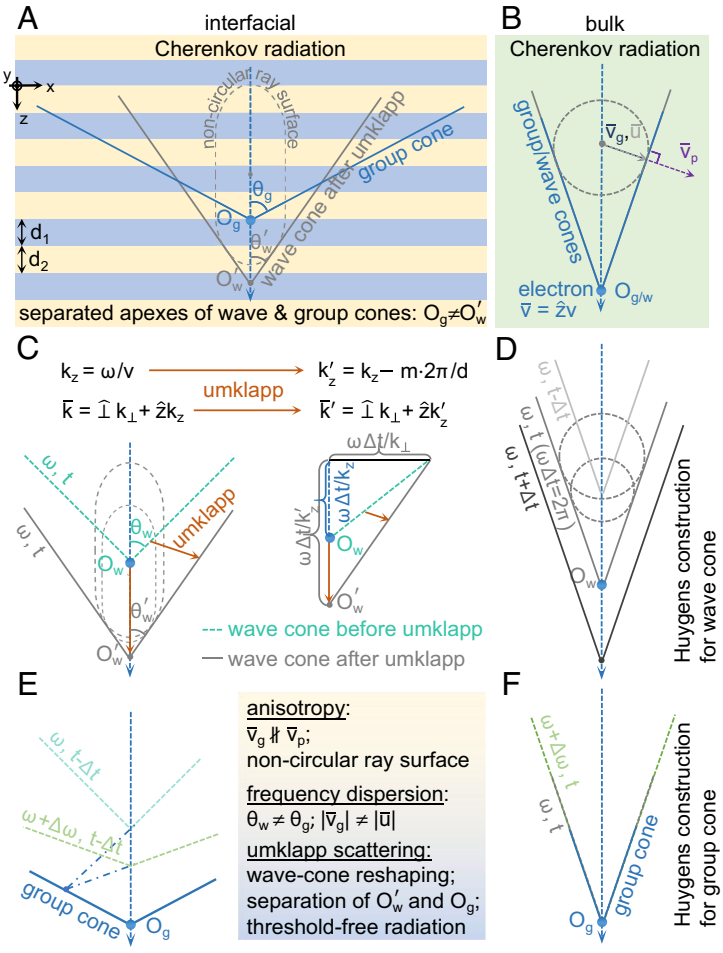

Fig. 1. Huygens construction of interfacial Cherenkov radiation with umklapp scattering inside an infinitely large one-dimensional photonic crystal. The photonic crystal is composed of two transparent materials with relative permittivities of $\varepsilon_{r,1}$ and $\varepsilon_{r,2}$ and thicknesses of d_1 and d_2, respectively. The Huygens construction of wave and group cones is related to four velocities, namely the electron velocity $\bar{v} = \hat{z}v$, the phase velocity $\bar{v}_p$, the group velocity $\bar{v}_g$, and the ray velocity $\bar{u}$. (*A*, *C*, and *E*) Interfacial Cherenkov radiation. (*B*, *D*, and *F*) Conventional bulk Cherenkov radiation inside an isotropic material without dispersion. The generatrix of the wave cone for monochromatic waves in *C* and *D* can be constructed by plotting the common tangent of Huygens wavelets with a same frequency ω emitted at different times. Since the monochromatic waves are radiated not in pulse, but continuously, there would be a series of wave cones whose generatrices are parallel to each other; see the instant positions of a series of wave cones with phase difference of $\omega\Delta t = 2\pi$ in *D*. The intersections of all wave-cone generatrices for two neighboring frequencies ω and $\omega + \Delta\omega$ would give the instant surface of equal phases for these two frequencies, namely the instant position of group cone in *E* and *F*, where $\Delta\omega/\omega \to 0$. From the causality principle, the apex of the group cone always coincides with the instant position of the moving electron. Due to the umklapp scattering, the wave cone would be reshaped, including its apex and aperture.

velocity $\overline{v} = \hat{z}v$, the group velocity $\overline{v}_g = \hat{\perp}v_{g,\perp} + \hat{z}v_{g,z}$, the phase velocity $\overline{v}_p = \hat{k}v_p = \hat{\perp}v_{p,\perp} + \hat{z}v_{p,z}$, and the ray velocity $\overline{u} = \hat{\perp}u_\perp + \hat{z}u_z$, where $\hat{\perp}$ is a basis vector perpendicular to the electron velocity. The electron's velocity would be below the Cherenkov threshold by imposing the constraint of $v < min\left(c/\sqrt{\varepsilon_{r,1}}, c/\sqrt{\varepsilon_{r,2}}\right)$ in Fig. 1 *A*, *C*, and *E*; as a result, the possibility of conventional bulk Cherenkov radiation inside the photonic crystal is excluded. The group velocity in this work maintains its physical meaning as the velocity of energy flow (63, 64), since there is no anomalous dispersion in our studied system. While the phase velocity $\overline{v}_p = \hat{k}v_p$ represents the velocity of phase propagation along the wavevector $\overline{k}$ of the emitted light, the ray velocity corresponds to the velocity of phase propagation along the ray, namely along the direction of energy flow (61, 62). Mathematically, we have $\hat{k} \cdot \overline{u} = v_p$ and $\overline{u} \| \overline{v}_g$ (60–62).

Due to the anisotropy of photonic crystals, the phase velocity and group velocity of Bloch modes are nonparallel, and a noncircular ray surface is formed for all Bloch modes and thus the secondary Huygens wavelets at a given frequency in Fig. 1*A*. With the knowledge of ray surface (60, 65), the wave cone with an aperture θ_w can be constructed by the common tangent of secondary Huygens wavelets in Fig. 1*C*, where $\theta_w = \arctan\left(\frac{u_\perp}{v-u_z}\right) = \arcsin\left(\frac{v_p}{v}\right)$ is related to either the ray or phase velocity (*SI Appendix*, section S3). Correspondingly, the intersection of all wave-cone generatrices for two neighboring frequencies would determine the instant position of the group cone with an aperture θ_g in Fig. 1*E*, where $\theta_g = \arctan\left(\frac{v_{g,\perp}}{v-v_{g,z}}\right)$ is related to the group velocity. Due to the frequency dispersion of photonic crystals, we generally have nonidentical magnitudes for the ray and group velocities, namely $|\overline{u}| \neq |\overline{v}_g|$. As a result, the apertures for the wave and group cones are generally not identical, namely $\theta_g \neq \theta_w$. Since these properties are purely induced by the anisotropy and the frequency dispersion, they are not unique to the interfacial Cherenkov radiation but in principle can occur for the conventional bulk Cherenkov radiation, for example, inside an anisotropic material with the presence of frequency dispersion (62, 66, 67). For comparison, we also show the Huygens construction for conventional bulk Cherenkov radiation inside an isotropic material with a relative permittivity of $\varepsilon_r = \varepsilon_{r,2}$ in Fig. 1 *B*, *D*, and *F*. Due to the isotropy and the absence of frequency dispersion, the bulk Cherenkov radiation has a circular ray surface for the secondary Huygens wavelets, $\overline{v}_p = \overline{v}_g = \overline{u}$, and $\theta_g = \theta_w$.

The interfacial Cherenkov radiation from low-energy electrons is always accompanied by the umklapp scattering due to the structural periodicity of photonic crystals. The umklapp scattering plays a critical role in reshaping the wave cone of interfacial Cherenkov radiation in Fig. 1*C*, including its aperture and apex. In the absence of the umklapp scattering, the emitted Bloch mode has a wavevector of $\overline{k} = \hat{\perp}k_\perp + \hat{z}k_z$, where $k_z = \omega/v$ is determined by the electron velocity according to the phase matching condition between the emitted light and the moving electron. Correspondingly, the original wave cone has an aperture of $\theta_w = \arcsin\left(\frac{v_p}{v}\right) = \arctan\left(\frac{k_z}{k_\perp}\right)$, and the apex of each wave cone moves with a velocity of $\overline{v}_{apex,w} = \frac{\hat{z}\omega}{k_z} = \hat{z}v = \overline{v}$. Since $\overline{v}_{apex,w}$ is equal to the electron velocity, the apex O_w of one specific wave cone could be spatially overlapped with the moving electron at any time. Due to the umklapp scattering along the periodicity direction, the z-component of wavevector would be changed from k_z to $k'_z = k_z - m \cdot 2\pi/d$, where d is the unit-cell thickness of photonic crystals and the Fourier order m is a nonzero integer. As a result, the excited Bloch mode after the umklapp scattering has a wavevector of $\overline{k}' = \hat{\perp}k_\perp + \hat{z}k'_z$. Then, each wave cone would be reshaped to have an aperture of $\theta'_w = \arctan\left(\frac{k'_z}{k_\perp}\right)$. Moreover, the apex of each wave cone would be reshaped to move with a velocity of $\overline{v}'_{apex,w} = \hat{z}\omega/k'_z$. Because $\overline{v}'_{apex,w} \neq \overline{v}$, the apexes of all wave cones would be spatially separated from the moving electron as the time varies. For example, the apex O_w is reshaped to O'_w, whose position is ahead of the moving electron in Fig. 1*C*. These modifications to the wave cone do not violate the causality principle (65) because the wave cone does not necessarily carry the radiated energy.

On the other hand, the group cone of interfacial Cherenkov radiation would not undergo the umklapp scattering, as fundamentally governed by the causality principle. Correspondingly, the Huygens construction of the group cone in Fig. 1*E* should use the original wave cones before the umklapp scattering. In other words, the apex of the group cone should always be spatially overlapped with the position of the moving electron and moves with a velocity of $\overline{v}_{apex,g} = \overline{v}$, since the group cone is related to the propagation of the radiated energy which emanates from the moving electron. While the interfacial Cherenkov radiation has $\overline{v}_{apex,g} \neq \overline{v}'_{apex,w}$, there exists no such a reshaped wave cone after the umklapp scattering whose apex is overlapped with that of the group cone at any time, namely $O_g \neq O'_w$.

To facilitate the understanding of interfacial Cherenkov radiation, we show the spatial distribution of excited fields when an electron moves inside an infinitely large photonic crystal in Fig. 2 *A* and *C* and an infinitely-large homogeneous material in Fig. 2 *B* and *D*. At the frequency domain, the field $D_z(\omega)$ is shown in Fig. 2 *A* and *B*. Plane-like waves are created inside both the photonic crystal and the homogeneous material, which represent a direct signature for the emergence of Cherenkov radiation. This way, Fig. 2 *A* and *B* indicate that the constructive interference of light emission from particle–interface interactions could offer an alternative way to create the Cherenkov radiation, in addition to particle–bulk interactions. At the time domain in Fig. 2 *C* and *D*, the field $D_z(t) = \int d\omega D_z(\omega) e^{-i\omega t} F_{win}(\omega)$ is calculated in Fig. 2 *C* and *D*, where a window function $F_{win}(\omega)$ is used to get a clear picture of the group cone. Since $\overline{v}_{apex,g} \neq \overline{v}'_{apex,w}$, the interfacial Cherenkov radiation in Fig. 2*C* has spatially separated apexes for its wave cone after the umklapp scattering and its group cone (namely $O_g \neq O'_w$), and it is distinct from the conventional bulk Cherenkov radiation ($O_g = O_w$) in Fig. 2*D*.

To consider the potential influence of reflection at the interface of photonic crystals, we further investigate the interfacial Cherenkov radiation from a photonic crystal with a finite length in Figs. 3 and 4. The photonic crystal is surrounded by free space, and it has a unit-cell number of 200 in Figs. 3 and 4. For the interfacial Cherenkov radiation, the corresponding momentum mismatch and the total internal reflection could be avoided by imposing the constraint of $|k_\perp| \leq k_0$, where k_0 is the wavevector of emitted light into free space. By enforcing the boundary conditions, we have the radiation angle $\theta = \arcsin\left(\frac{|k_\perp|}{k_0}\right)$, which is the angle between $\overline{k}$ and $\overline{v}$ ($-\overline{v}$) for the forward (backward) radiation as schematically shown in Fig. 3*A*. Under this scenario, we

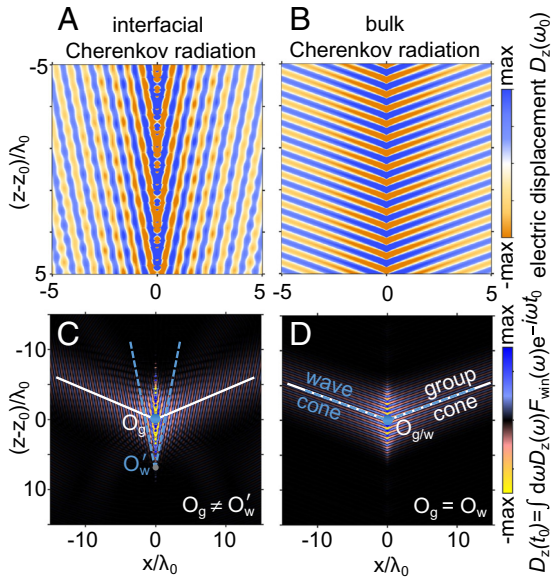

Fig. 2. Real-space demonstration of wave and group cones for interfacial Cherenkov radiation inside an infinitely large photonic crystal. The structural setup of the photonic crystal is $\varepsilon_{r,1} = 2.1$, $\varepsilon_{r,2} = 2.3$, $d_1 = 0.3\lambda_0$, and $d_2 = 0.7\lambda_0$, where λ_0 is working wavelength in free space. For the interfacial Cherenkov radiation in the left panel, the electron velocity of $v = 0.4c < \min\left(c/\sqrt{\varepsilon_{r,1}}, c/\sqrt{\varepsilon_{r,2}}\right)$ is used. That is, this electron velocity is chosen to be below the Cherenkov threshold and the corresponding kinetic energy is 46.5 keV. For the bulk Cherenkov radiation in the *Right* panel, an isotropic material with a relative permittivity of $\varepsilon_r = \varepsilon_{r,2}$ and the electron velocity of $v = 0.7c > c/\sqrt{\varepsilon_r}$ are used. That is, this electron velocity is chosen to be above the Cherenkov threshold and the corresponding kinetic energy is 205 keV. The instant position of the electron is at $z = z_0$ for the time of $t = t_0$. (*A* and *B*) Distribution of excited field $D_z(\omega_0)$. Plane-like waves are induced both for the interfacial and bulk Cherenkov radiation. (*C* and *D*) Distribution of excited field $D_z(t_0) = \int d\omega D_z(\omega) e^{-i\omega t_0} F_{win}(\omega)$, where a window function $F_{win}(\omega) = e^{-\frac{\sigma_z^2(\omega-\omega_0)^2}{2v^2}}$ with $\sigma_z = 2.5\lambda_0$ is used for the illustration of the group cone.

find the relationship between the electron velocity $\overline{v}$ and the radiation angle θ is governed by

$$v = \frac{\omega d}{2m\pi + \phi(\theta, \omega)} \quad [1]$$

$$\phi(\theta,\omega) = \arccos\left[\cos k_{z,1}d_1 \cos k_{z,2}d_2 - \frac{1}{2}\sin\left(k_{z,1}d_1\right)\right.$$
$$\left.\sin\left(k_{z,2}d_2\right)\left(\frac{\varepsilon_{r,1}k_{z,2}}{\varepsilon_{r,2}k_{z,1}} + \frac{\varepsilon_{r,2}k_{z,1}}{\varepsilon_{r,1}k_{z,2}}\right)\right] \quad [2]$$

where $d = d_1 + d_2$ is the unit-cell thickness of photonic crystals, d_j is the thickness of the photonic crystal constituent with $\varepsilon_{r,j}$, $k_{z,j} = k_0\sqrt{\varepsilon_{r,j} - \sin^2\theta}$, and j is either 1 or 2.

The factor of $2m\pi$ in Eq. **1** stems exactly from the umklapp scattering, whose existence ensures the possible solution of θ in Eq. **1** even under the scenario of $v/c \ll 1$, where c is the speed of light in free space. In other words, the interfacial Cherenkov radiation is in principle threshold-free, as can be seen from the dependence of the radiation angle on the electron velocity in Fig. 3 *B* and *C*. For example, the interfacial Cherenkov radiation could occur even when the electron velocity is down to the order of $10^{-2}c$ in Fig. 3*C*, due to the umklapp scattering with $m = 45$ for high-k Bloch modes (or down to the order of $10^{-3}c$ with $m = 900$ in *SI Appendix*, Fig. S8).

To rigorously demonstrate the angular feature of interfacial Cherenkov radiation, its total angular spectral energy density $U_{\text{total}}(\theta, v)$ is shown in Fig. 3*D* by following and extending Ginzburg and Frank's theory of transition radiation within the framework of classic electromagnetic wave theory (13, 51, 52, 68–72). In principle, our results do not depend on the specific choice of working angular frequency ω, as long as the emitted photon energy $\hbar\,\hbar\omega$ is much smaller than the kinetic energy E_k of electrons, namely $\hbar\,\hbar\omega \ll E_k$, so that the quantum recoil effect (48) can be safely neglected. The interfacial Cherenkov radiation with high directionality from ultralow-energy electrons manifests itself as the radiation peaks in the θ -v parameter space. Moreover, the trajectory of these radiation peaks in Fig. 3*D* is in accordance with the relationship between θ and v as revealed in Fig. 3*C*, which proves the validity of Eq. **1**. On the other hand, there are regions in the θ–v parameter space with the absence of interfacial Cherenkov radiation in Fig. 3 *B* and *D*. This is due to the failure of forming the constructive interference of light emission from particle–interface interactions. This way, the free-electron radiation in these regions still behaves as the conventional transition radiation and suffers from the low directionality and the low intensity in Fig. 3*D*.

Moreover, we find that the interfacial Cherenkov radiation has a certain tolerance to the variation of material's permittivity in *SI Appendix*, Fig. S4, the variation of the thickness of each constituent dielectric layer in *SI Appendix*, Fig. S5, and the material loss in *SI Appendix*, Fig. S6. Meanwhile, the photon extraction efficiency (26, 70) of interfacial Cherenkov radiation would exhibit a periodic oscillation tendency with respect to the order of umklapp scattering or the electron velocity in *SI Appendix*, Fig. S7. In addition, when considering the energy bandwidth of free electrons, there could be an angular spread of the interfacial Cherenkov radiation in *SI Appendix*, Fig. S11.

Last but not least, the combined effect of umklapp scattering and particle–interface interactions could also enable the possibility of creating the backward Cherenkov radiation, as shown in Fig. 4 *A*–*D*. While the backward Cherenkov radiation has been extensively demonstrated from optical systems with an effective negative index or $\overline{v}_p \cdot \overline{v}_g < 0$ (66, 73–75), our revealed one from ultralow-energy electrons (e.g., with $v/c \ll 1$) that has no momentum mismatch with light in free space in Fig. 4 and *SI Appendix*, Fig. S9 has never been reported before.

While the relation between θ and v for the interfacial Cherenkov radiation could be well predicted from Eq. **1** or the result in Fig. 3*B*, the direction of its energy flow inside the photonic crystal is still elusive. To address this issue, the angular spectral energy density for the forward radiation $U_F(\theta, v)$ and the backward radiation $U_B(\theta, v)$ are separately plotted in Fig. 4 *A* and *B*, respectively. From Fig. 4 *A* and *B*, the predominant energy flow of interfacial Cherenkov radiation would propagate in opposite directions in different regimes of the electron velocity. The forward interfacial Cherenkov radiation is characterized by $U_F(\theta, v) \gg U_B(\theta, v)$ in Fig. 4*A*, and the originally excited interfacial Cherenkov radiation inside the photonic crystal propagates along the $+z$ direction in Fig. 4*C*. By contrast, the backward interfacial Cherenkov radiation begins to have $U_F(\theta, v) \ll U_B(\theta, v)$, and it propagates along the $-z$ direction inside the photonic crystal in Fig. 4*D*.

In conclusion, we have revealed that the combined effect of umklapp scattering and particle–interface interactions could provide a viable mechanism to create the interfacial Cherenkov radiation from ultralow-energy electrons that has no momentum mismatch with light in free space. This combined effect also enables a viable route to create the backward interfacial

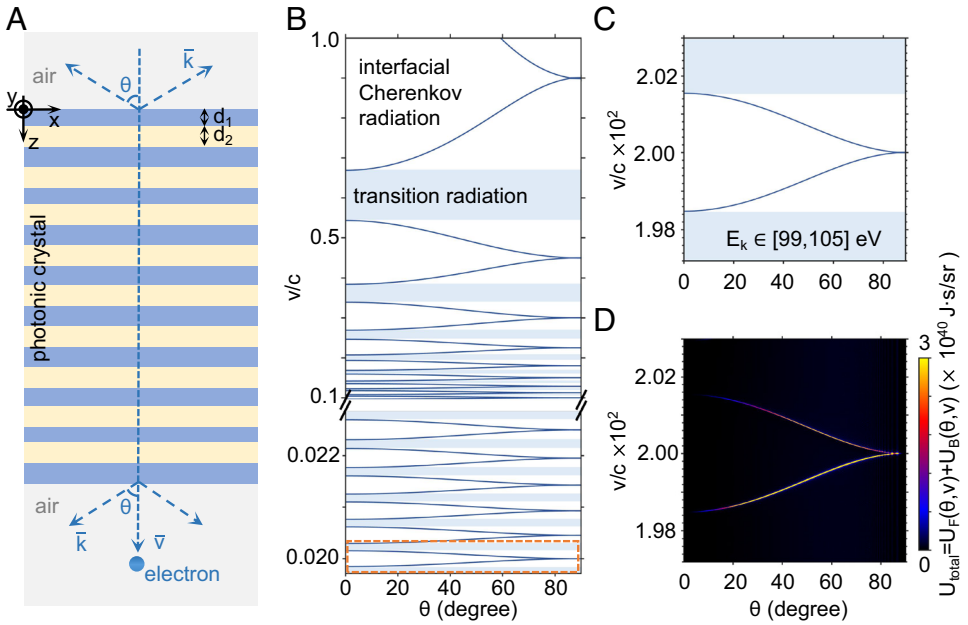

Fig. 3. Interfacial Cherenkov radiation from an ultralow-energy electron perpendicularly penetrating a photonic crystal with a finite thickness. The structural setup of the photonic crystal is the same as that in Fig. 2. (*A*) Structural schematic. The radiation θ is the angle between $\bar{v}$ ($-\bar{v}$) and $\bar{k}$ for the forward (backward) radiation. (*B* and *C*) Relation between the radiation angle of interfacial Cherenkov radiation and the electron velocity. The ultralow-velocity regime in *B* as highlighted by the orange dashed line is enlarged and replotted in *C*. (*D*) $U_{\text{total}} = U_B(\theta, v) + U_F(\theta, v)$ as a function of the electron velocity and the radiation angle, where $U_F(\theta, v)$ and $U_B(\theta, v)$ represent the angular spectral energy densities of the forward and backward radiation, respectively. The velocity range of $v/c \in [1.97, 2.03] \times 10^{-2}$ in (*C* and *D*) corresponds to the electron kinetic energy of $E_k \in [99, 105]$ eV. This velocity range is chosen to show the possibility of creating the interfacial Cherenkov radiation from low-energy electrons.

Cherenkov radiation from ultralow-energy electrons that can freely couple into free space. Moreover, we have found that the interfacial Cherenkov radiation is uniquely featured with spatially separated apexes for its wave and group cones, as intrinsically governed by the umklapp scattering for high-momentum Bloch modes. The revealed interfacial Cherenkov radiation may contribute to the development of compact on-chip light source from ultralow-energy electrons; see the discussion about integration and scalability of these light sources with enhanced photon exaction efficiency in *SI Appendix*, Figs. S12 and S13.

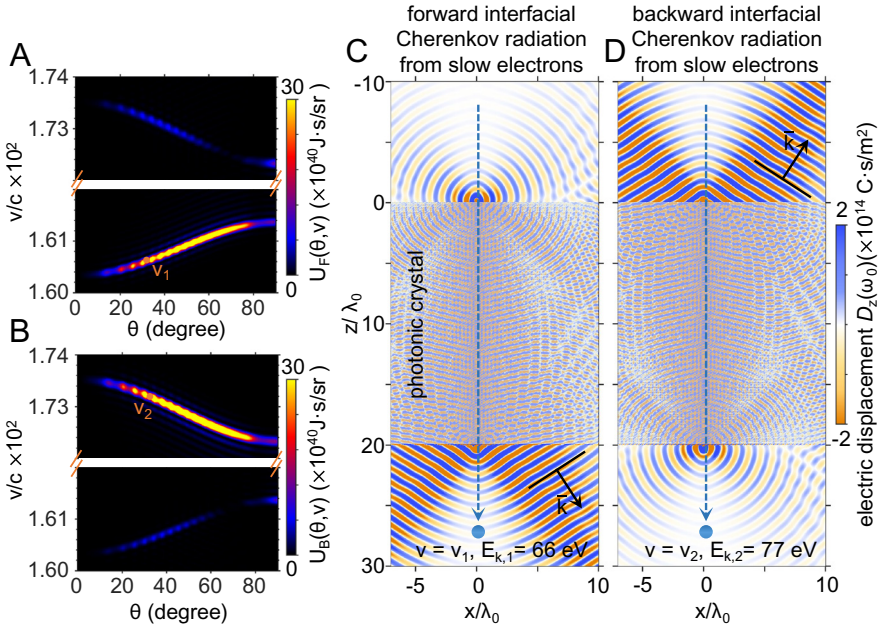

Fig. 4. Forward and backward interfacial Cherenkov radiation excited by low-energy electrons from a photonic crystal with a finite thickness. (*A*) Angular spectral energy density $U_F(\theta, v)$ of the forward free-electron radiation. (*B*) Angular spectral energy density $U_B(\theta, v)$ of the backward free-electron radiation. (*C*) Effective forward interfacial Cherenkov radiation, under the condition that the electron velocity is $v = v_1$, whose corresponding kinetic energy is $E_{k,1} = 66$ eV. (*D*) Effective backward interfacial Cherenkov radiation under the condition that the electron velocity is $v = v_2$, whose corresponding kinetic energy is $E_{k,2} = 77$ eV. These two electron velocities are chosen to demonstrate the possibility to create the forward or backward interfacial Cherenkov radiation from ultralow-energy electrons.

Materials and Methods

Deviation of Interfacial Cherenkov Radiation. Within the classical electromagnetic wave theory, we follow and extend Ginzburg and Frank's theory of transition radiation from a single interface to a multilayered system with N interfaces and $N+1$ regions, as schematically illustrated in *SI Appendix*, Fig. S1. The excited field distribution and angular spectral energy density are analytically derived in *SI Appendix*, section S1. To be specific, the field distribution in real space can be derived by performing the plane-wave expansion, that is, $\bar{E}^R(\bar{r},t)=\int d\omega d\bar{k}_\perp E^R_{\bar{k}_\perp,\omega}\, e^{i\bar{k}_\perp\bar{r}_\perp-i\omega t}$. In $\bar{k}_\perp$ and ω spaces, the distribution of radiation field in region j is obtained as

$$E^R_{\bar{k}_\perp,\omega,z,j}=\begin{cases}\dfrac{iq}{\omega\varepsilon_0(2\pi)^3}\cdot a_1\cdot e^{-ik_{z,1}(z-d_1)} & (j=1)\\ \dfrac{iq}{\omega\varepsilon_0(2\pi)^3}\left[a_j^-\cdot e^{-ik_{z,j}(z-d_j)}+a_j^+\cdot e^{ik_{z,j}(z-d_{j-1})}\right] & (2\le j\le N)\\ \dfrac{iq}{\omega\varepsilon_0(2\pi)^3}\cdot a_{N+1}\cdot e^{ik_{z,N+1}(z-d_N)} & (j=N+1)\end{cases}$$

where a_j^- (a_j^+) is the generalized factor for the backward (forward) radiation in region j, which contains the information of interference of transition radiation from multiple interfaces. Based on the knowledge of the radiation field, the backward angular spectral energy density is obtained as $U_B(\theta,v)=\frac{\varepsilon_{r,1}^{3/2}q^2\cos^2\theta|a_1|^2}{4\pi^3\varepsilon_0 c\sin^2\theta}$, and the forward angular spectral energy density is obtained as $U_F(\theta,v)=\frac{\varepsilon_{r,N+1}^{3/2}q^2\cos^2\theta|a_{N+1}|^2}{4\pi^3\varepsilon_0 c\sin^2\theta}$. Moreover, the numerical calculation of excited fields of interfacial Cherenkov radiation can be obtained with the aid of Sommerfeld integration.

More Discussion about Huygens Construction for Interfacial Cherenkov Radiation. Huygens wavelets have the shape of the ray surface and can be constructed with the knowledge of the wave-vector surface. The connection between the ray surface and the wave-vector surface is illustrated in *SI Appendix*, Fig. S2. Physical interpretation of the ray velocity and its connection with the group velocity are discussed in *SI Appendix*, section S2.

Aperture of Group Cone for the Interfacial Cherenkov Radiation. The aperture of group cone for the interfacial Cherenkov radiation is related to the group velocity $\bar{v}_g$, while the aperture of wave cone is related to the ray velocity $\bar{u}$ or the phase velocity $\bar{v}_p$. The detailed derivation is provided in *SI Appendix*, section S3 and Fig. S3.

Correspondence between Radiation Angle and Electron Velocity. We provide the detailed derivation for Eqs. **1** and **2** in *SI Appendix*, section S4.

More Discussion on the Interfacial Cherenkov Radiation. We provide more discussion on the analyses of interfacial Cherenkov radiation in *SI Appendix*, section S5. The analyses include the influence of the variation of material's permittivity and the thickness of the constituent dielectric layer on the interfacial Cherenkov radiation in *SI Appendix*, Figs. S4 and S5, the influence of material loss on the interfacial Cherenkov radiation in *SI Appendix*, Fig. S6, correlations between the order of umklapp scattering and the photon exaction efficiency in *SI Appendix*, Fig. S7, more cases of interfacial Cherenkov radiation from ultralow-energy electrons in *SI Appendix*, Figs. S8 and S9, discussion on the quantum recoil effect and radiation efficiency in *SI Appendix*, Fig. S10, influence of electron's energy bandwidth on the interfacial Cherenkov radiation in *SI Appendix*, Fig. S11, and integration and scalability of interfacial-Cherenkov-radiation-based light sources with enhanced photon exaction efficiency in *SI Appendix*, Figs. S12 and S13.

Data, Materials, and Software Availability. All theoretical and numerical findings can be reproduced based on the information in the article and/or *SI Appendix*. The data represented in all Figures is available on https://doi.org/10.5281/zenodo.8284340 (76).

ACKNOWLEDGMENTS. X.L. acknowledges the support partly from the National Natural Science Fund for Excellent Young Scientists Fund Program (Overseas) of China, the National Natural Science Foundation of China under Grant No. 62175212, Zhejiang Provincial Natural Science Fund Key Project under Grant No. LZ23F050003, and the Fundamental Research Funds for the Central Universities (2021FZZX001-19). H.C. acknowledges the support from the Key Research and Development Program of the Ministry of Science and Technology under Grants Nos. 2022YFA1404704, 2022YFA1405200, and 2022YFA1404902, the National Natural Science Foundation of China under Grants No. 61975176, the Key Research and Development Program of Zhejiang Province under Grant No. 2022C01036, and the Fundamental Research Funds for the Central Universities. J.C. acknowledges the support from the Chinese Scholarship Council (CSC No. 202206320287). B.Z. acknowledges the support from Singapore National Research Foundation Competitive Research Program No. NRF-CRP23-2019-0007. Y.Y. acknowledges the support from the start-up fund of the University of Hong Kong and the National Natural Science Foundation of China Excellent Young Scientists Fund (HKU 12222417).

Author affiliations: [a]Interdisciplinary Center for Quantum Information, State Key Laboratory of Extreme Photonics and Instrumentation, ZJU-Hangzhou Global Scientific and Technological Innovation Center, Zhejiang University, Hangzhou 310027, China; [b]International Joint Innovation Center, The Electromagnetics Academy at Zhejiang University, Zhejiang University, Haining 314400, China; [c]Department of Electrical and Computer Engineering, Technion-Israel Institute of Technology, Haifa 32000, Israel; [d]School of Physics, Zhejiang University, Hangzhou 310027, China; [e]Key Laboratory of Advanced Micro/Nano Electronic Devices & Smart Systems of Zhejiang, Jinhua Institute of Zhejiang University, Zhejiang University, Jinhua 321099, China; [f]College of Electronic and Information Engineering, Nanjing University of Aeronautics and Astronautics, Nanjing 211106, China; [g]Department of Physics, University of Hong Kong, Hong Kong 999077, China; [h]Division of Physics and Applied Physics, School of Physical and Mathematical Sciences, Nanyang Technological University, Singapore 637371, Singapore; [i]Centre for Disruptive Photonic Technologies, Nanyang Technological University, Singapore 637371, Singapore; and [j]Shaoxing Institute of Zhejiang University, Zhejiang University, Shaoxing 312000, China

1. P. A. Cherenkov, Visible emission of clean liquids by action of gamma radiation. *Dokl. Akad. Nauk SSSR* **2**, 451–454 (1934).
2. C. Roques-Carmes *et al.*, Free-electron-light interactions in nanophotonics. *Appl. Phys. Rev.* **10**, 011303 (2023).
3. Y. Adiv *et al.*, Observation of 2D Cherenkov radiation. *Phys. Rev. X* **13**, 011002 (2023).
4. Y. Yang *et al.*, Photonic flatband resonances for free-electron radiation. *Nature* **613**, 42–47 (2023).
5. A. Dikopoltsev *et al.*, Light emission by free electrons in photonic time-crystals. *Proc. Natl. Acad. Sci. U.S.A.* **119**, e2119705119 (2022).
6. H. Hu *et al.*, Surface Dyakonov–Cherenkov radiation. *eLight* **2**, 2 (2022).
7. P. Genevet *et al.*, Controlled steering of Cherenkov surface plasmon wakes with a one-dimensional metamaterial. *Nat. Nanotechnol.* **10**, 804–809 (2015).
8. O. Chamberlain, E. Segrè, C. Wiegand, T. Ypsilantis, Observation of antiprotons. *Phys. Rev.* **100**, 947–950 (1955).
9. J. J. Aubert *et al.*, Experimental observation of a heavy particle. *J. Phys. Rev. Lett.* **33**, 1404–1406 (1974).
10. M. Amenomori *et al.*, First detection of sub-PeV diffuse gamma rays from the galactic disk: Evidence for ubiquitous galactic cosmic rays beyond PeV energies. *Phys. Rev. Lett.* **126**, 141101 (2021).
11. X. Lin *et al.*, A Brewster route to Cherenkov detectors. *Nat. Commun.* **12**, 5554 (2021).
12. M. Adinolfi *et al.*, Performance of the LHCb RICH detector at the LHC. *Eur. Phys. J. C* **73**, 2431 (2013).
13. X. Lin *et al.*, Controlling Cherenkov angles with resonance transition radiation. *Nat. Phys.* **14**, 816–821 (2018).
14. G. Adamo *et al.*, Light well: A tunable free-electron light source on a chip. *Phys. Rev. Lett.* **103**, 113901 (2009).
15. S. Liu *et al.*, Surface polariton Cherenkov light radiation source. *Phys. Rev. Lett.* **109**, 153902 (2012).
16. F. Liu *et al.*, Integrated Cherenkov radiation emitter eliminating the electron velocity threshold. *Nat. Photon.* **11**, 289–292 (2017).
17. R. L. Hachadorian *et al.*, Imaging radiation dose in breast radiotherapy by X-ray CT calibration of Cherenkov light. *Nat. Commun.* **11**, 2298 (2020).
18. D. A. Alexander *et al.*, Color Cherenkov imaging of clinical radiation therapy. *Light Sci. Appl.* **10**, 226 (2021).
19. T. M. Shaffer, E. C. Pratt, J. Grimm, Utilizing the power of Cerenkov light with nanotechnology. *Nat. Nanotechnol.* **12**, 106–117 (2017).
20. X. Wang *et al.*, Cherenkov luminescence in tumor diagnosis and treatment: A review. *Photonics* **9**, 390 (2022).
21. N. Kotagiri, G. P. Sudlow, W. J. Akers, S. Achilefu, Breaking the depth dependency of phototherapy with Cerenkov radiation and low-radiance-responsive nanophotosensitizers. *Nat. Nanotechnol.* **10**, 370–379 (2015).
22. A. Kamkaew *et al.*, Cerenkov radiation induced photodynamic therapy using chlorin e6-loaded hollow mesoporous silica nanoparticles. *ACS Appl. Mater. Interfaces* **8**, 26630–26637 (2016).
23. I. E. Tamm, I. M. Frank, Coherent radiation of fast electrons in a medium. *Dokl. Akad. Nauk SSSR* **14**, 107–112 (1937).
24. I. Tamm, Radiation emitted by uniformly moving electrons. *J. Phys. (USSR)* **1**, 439–454 (1939).

25. I. Kaminer *et al.*, Efficient plasmonic emission by the quantum Čerenkov effect from hot carriers in graphene. *Nat. Commun.* **7**, 11880 (2016).
26. A. Massuda *et al.*, Smith–Purcell radiation from low-energy electrons. *ACS Photonics* **5**, 3513–3518 (2018).
27. Y.Y. Auad *et al.*, μeV electron spectromicroscopy using free-space light. *Nat. Commun.* **14**, 4442 (2023).
28. N. Talebi, Strong interaction of slow electrons with near-field light visited from first principles. *Phys. Rev. Lett.* **125**, 080401 (2020).
29. M. Eldar, Y. Pan, M. Krüger, Self-trapping of slow electrons in the energy domain. arXiv [Preprint] (2022). https://doi.org/10.48550/arXiv.2209.14850 (Accessed 10 April 2023).
30. Y. Hochberg *et al.*, Determining dark-matter–electron scattering rates from the dielectric function. *Phys. Rev. Lett.* **127**, 151802 (2021).
31. T. Zhang *et al.*, Tunable optical topological transition of Cherenkov radiation. *Photonics Res.* **10**, 1650–1660 (2022).
32. H. Hu *et al.*, Nonlocality induced Cherenkov threshold. *Laser Photon. Rev.* **14**, 2000149 (2020).
33. A. A. Orlov, P. M. Voroshilov, P. A. Belov, Y. S. Kivshar, Engineered optical nonlocality in nanostructured metamaterials. *Phys. Rev. B* **84**, 045424 (2011).
34. W. Yan, M. Wubs, N. A. Mortensen, Hyperbolic metamaterials: Nonlocal response regularizes broadband supersingularity. *Phys. Rev. B* **86**, 205429 (2012).
35. L. Shen *et al.*, Broadband enhancement of on-chip single-photon extraction via tilted hyperbolic metamaterials. *Appl. Phys. Rev.* **7**, 021403 (2020).
36. D. Lu, J. J. Kan, E. E. Fullerton, Z. Liu, Enhancing spontaneous emission rates of molecules using nanopatterned multilayer hyperbolic metamaterials. *Nat. Nanotechnol.* **9**, 48–53 (2014).
37. T. Galfsky, J. Gu, E. E. Narimanov, V. M. Menon, Photonic hypercrystals for control of light–matter interactions. *Proc. Natl. Acad. Sci. U.S.A.* **114**, 5125–5129 (2017).
38. T. Galfsky *et al.*, Active hyperbolic metamaterials: Enhanced spontaneous emission and light extraction. *Optica* **2**, 62–65 (2015).
39. A. Poddubny, I. Iorsh, P. Belov, Y. Kivshar, Hyperbolic metamaterials. *Nat. Photon.* **7**, 948–957 (2013).
40. D. Lee *et al.*, Hyperbolic metamaterials: Fusing artificial structures to natural 2D materials. *eLight* **2**, 1 (2022).
41. N. v Sapra, *et al.*, On-chip integrated laser-driven particle accelerator. *Science* **367**, 79–83 (2020).
42. Y. Yang *et al.*, Maximal spontaneous photon emission and energy loss from free electrons. *Nat. Phys.* **14**, 894–899 (2018).
43. L. J. Wong, I. Kaminer, O. Ilic, J. D. Joannopoulos, M. Soljačić, Towards graphene plasmon-based free-electron infrared to X-ray sources. *Nat. Photon.* **10**, 46–52 (2016).
44. A. Polman, M. Kociak, F. J. G. de Abajo, Electron–beam spectroscopy for nanophotonics. *Nat. Mater.* **18**, 1158–1171 (2019).
45. M. Henstridge *et al.*, Synchrotron radiation from an accelerating light pulse. *Science* **362**, 439–442 (2018).
46. A. Feist *et al.*, Cavity-mediated electron-photon pairs. *Science* **377**, 777–780 (2022).
47. D. Zhang *et al.*, Coherent surface plasmon polariton amplification via free-electron pumping. *Nature* **611**, 55–60 (2022).
48. S. Huang *et al.*, Quantum recoil in free-electron interactions with atomic lattices. *Nat. Photon.* **17**, 224–230 (2023).
49. S. Tsesses *et al.*, Tunable photon-induced spatial modulation of free electrons. *Nat. Mater.* **22**, 345–352 (2023).
50. H. Hu, X. Lin, Y. Luo, Free-electron radiation engineering via structured environments. *Prog. Electromagn. Res.* **171**, 75–88 (2021).
51. V. L. Ginzburg, I. M. Frank, Radiation of a uniformly moving electron due to its transition from one medium into another. *J. Phys. (USSR)* **9**, 353–362 (1945).
52. V. L. Ginzburg, *Transition Radiation and Transition Scattering* (A. Hilger, 1990).
53. I. P. Ivanov, D. V. Karlovets, Detecting transition radiation from a magnetic moment. *Phys. Rev. Lett.* **110**, 264801 (2013).
54. R. Chen *et al.*, Recent advances of transition radiation: Fundamentals and applications. *Mater. Today Electron.* **3**, 100025 (2023).
55. C. Luo, M. Ibanescu, S. G. Johnson, J. D. Joannopoulos, Cerenkov radiation in photonic crystals. *Science* **299**, 368–371 (2003).
56. F. J. G. de Abajo, Optical excitations in electron microscopy. *Rev. Mod. Phys.* **82**, 209 (2010).
57. C. Kremers, D. N. Chigrin, J. Kroha, Theory of Cherenkov radiation in periodic dielectric media: Emission spectrum. *Phys. Rev. A* **79**, 013829 (2009).
58. C. Kremers, D. N. Chigrin, Spatial distribution of Cherenkov radiation in periodic dielectric media. *J. Opt. A* **11**, 114008 (2009).
59. F. J. G. de Abajo *et al.*, Cherenkov effect as a probe of photonic nanostructures. *Phys. Rev. Lett.* **91**, 143902 (2003).
60. A. Sommerfeld, *Optics* (Academic Press, 1954).
61. M. Born, E. Wolf, *Principles of Optics: Electromagnetic Theory of Propagation, Interference and Diffraction of Light* (Cambridge University Press, 1999).
62. I. M. Frank, On some peculiarities of Vavilov–Cherenkov radiation. *Nucl. Instrum. Methods Phys. Res. A* **248**, 7–12 (1986).
63. L. Brillouin, *Wave Propagation and Group Velocity* (Academic Press, 1960).
64. J. A. Stratton, *Electromagnetic Theory* (McGraw-Hill, 1941).
65. L. D. Landau, E. M. Lifshitz, *Electrodynamics of Continuous Media* (Pergamon, 1984).
66. H. Chen, M. Chen, Flipping photons backward: Reversed Cherenkov radiation. *Mater. Today* **14**, 34–41 (2011).
67. I. Carusotto, M. Artoni, G. C. la Rocca, F. Bassani, Slow group velocity and Cherenkov radiation. *Phys. Rev. Lett.* **87**, 064801 (2001).
68. X. Lin *et al.*, Splashing transients of 2D plasmons launched by swift electrons. *Sci. Adv.* **3**, e1601192 (2017).
69. J. Chen, H. Chen, X. Lin, Photonic and plasmonic transition radiation from graphene. *J. Opt.* **23**, 034001 (2021).
70. J. Chen *et al.*, Low-velocity-favored transition radiation. arXiv [Preprint] (2022). https://doi.org/10.48550/arXiv.2212.13066 (Accessed 2 January 2023).
71. F. Tay *et al.*, Bulk-Plasmon-Mediated Free-Electron Radiation Beyond the Conventional Formation Time. Advanced Science **10**, 2300760 (2023).
72. R. Chen *et al.*, Free-electron Brewster-transition radiation. *Sci. Adv.* **9**, eadh8098 (2023).
73. S. Xi *et al.*, Experimental verification of reversed Cherenkov radiation in left-handed metamaterial. *Phys. Rev. Lett.* **103**, 194801 (2009).
74. Z. Duan *et al.*, Observation of the reversed Cherenkov radiation. *Nat. Commun.* **8**, 14901 (2017).
75. V. G. Veselago, Electrodynamics of substances with simultaneously negative ε and μ. *Sov. Phys. Usp.* **10**, 509–514 (1968).
76. Z. Gong, Interfacial Cherenkov radiation from ultralow-energy electrons – Data set [Data set]. Zenodo. https://doi.org/10.5281/zenodo.8284340. Deposited 26 August 2023.